

# Observation of Beam Spin Asymmetries in the Process $ep \rightarrow e'\pi^+\pi^-X$ with CLAS12

T.B. Hayward,<sup>1</sup> C. Dils,<sup>2</sup> A. Vossen,<sup>2</sup> H. Avakian,<sup>3</sup> S. Adhikari,<sup>4</sup> G. Angelini,<sup>5</sup> M. Arratia,<sup>6,3</sup> H. Atac,<sup>7</sup> C. Ayerbe Gayoso,<sup>1</sup> N.A. Baltzell,<sup>3</sup> L. Barion,<sup>8</sup> M. Battaglieri,<sup>3,9</sup> I. Bedlinskiy,<sup>10</sup> F. Benmokhtar,<sup>11</sup> A. Bianconi,<sup>12,13</sup> A.S. Biselli,<sup>14</sup> M. Bondi,<sup>9</sup> F. Bossù,<sup>15</sup> S. Boiarinov,<sup>3</sup> W.J. Briscoe,<sup>5</sup> W.K. Brooks,<sup>16</sup> D. Bulumulla,<sup>17</sup> V.D. Burkert,<sup>3</sup> D.S. Carman,<sup>3</sup> J.C. Carvajal,<sup>4</sup> A. Celentano,<sup>9</sup> P. Chatagnon,<sup>18</sup> T. Chetry,<sup>19,20</sup> G. Ciullo,<sup>8,21</sup> B.A. Clary,<sup>22</sup> P.L. Cole,<sup>23</sup> M. Contalbrigo,<sup>8</sup> G. Costantini,<sup>12,13</sup> V. Crede,<sup>24</sup> A. D'Angelo,<sup>25,26</sup> N. Dashyan,<sup>27</sup> R. De Vita,<sup>9</sup> M. Defurne,<sup>15</sup> A. Deur,<sup>3</sup> S. Diehl,<sup>28,22</sup> C. Djalali,<sup>20</sup> R. Dupre,<sup>18</sup> M. Dugger,<sup>29</sup> H. Egiyan,<sup>3</sup> M. Ehrhart,<sup>30,18</sup> A. El Alaoui,<sup>16</sup> L. El Fassi,<sup>19</sup> L. Elouadrhiri,<sup>3</sup> S. Fegan,<sup>31</sup> A. Filippi,<sup>32</sup> T.A. Forest,<sup>33</sup> G. Gavalian,<sup>3</sup> G.P. Gilfoyle,<sup>34</sup> F.X. Girod,<sup>3</sup> D.I. Glazier,<sup>35</sup> A.A. Golubenko,<sup>36</sup> R.W. Gothe,<sup>37</sup> Y. Gotra,<sup>3</sup> K.A. Griffioen,<sup>1</sup> M. Guidal,<sup>18</sup> K. Hafidi,<sup>30</sup> H. Hakobyan,<sup>16,27</sup> M. Hattawy,<sup>17</sup> K. Hicks,<sup>20</sup> A. Hobart,<sup>18</sup> M. Holtrop,<sup>38</sup> D.G. Ireland,<sup>35</sup> E.L. Isupov,<sup>36</sup> H.S. Jo,<sup>39</sup> K. Joo,<sup>22</sup> S. Joosten,<sup>30</sup> D. Keller,<sup>40</sup> M. Khachatryan,<sup>17</sup> A. Khanal,<sup>4</sup> A. Kim,<sup>22</sup> W. Kim,<sup>39</sup> A. Kripko,<sup>28</sup> V. Kubarovsky,<sup>3</sup> S.E. Kuhn,<sup>17</sup> L. Lanza,<sup>25</sup> M. Leali,<sup>12,13</sup> S. Lee,<sup>41</sup> P. Lenisa,<sup>8,21</sup> K. Livingston,<sup>35</sup> I.J.D. MacGregor,<sup>35</sup> D. Marchand,<sup>18</sup> N. Markov,<sup>3,22</sup> L. Marsicano,<sup>9</sup> V. Mascagna,<sup>42,13,\*</sup> B. McKinnon,<sup>35</sup> Z.E. Meziani,<sup>30,7</sup> M. Mirazita,<sup>43</sup> V. Mokeev,<sup>3</sup> A. Movsisyan,<sup>8</sup> C. Munoz Camacho,<sup>18</sup> P. Nadel-Turonski,<sup>3</sup> P. Naidoo,<sup>35</sup> S. Nanda,<sup>19</sup> K. Neupane,<sup>37</sup> S. Niccolai,<sup>18</sup> G. Niculescu,<sup>44</sup> T.R. O'Connell,<sup>22</sup> M. Osipenko,<sup>9</sup> M. Paolone,<sup>45,7</sup> L.L. Pappalardo,<sup>8,21</sup> R. Paremuzyan,<sup>3,38</sup> E. Pasyuk,<sup>3</sup> W. Phelps,<sup>46</sup> O. Pogorelko,<sup>10</sup> Y. Prok,<sup>17</sup> B.A. Raue,<sup>4,3</sup> M. Ripani,<sup>9</sup> J. Ritman,<sup>47</sup> A. Rizzo,<sup>25,26</sup> P. Rossi,<sup>3,43</sup> J. Rowley,<sup>20</sup> F. Sabatié,<sup>15</sup> C. Salgado,<sup>48</sup> A. Schmidt,<sup>5</sup> E.P. Segarra,<sup>41</sup> Y.G. Sharabian,<sup>3</sup> U. Shrestha,<sup>20</sup> O. Soto,<sup>43,16</sup> N. Sparveris,<sup>7</sup> S. Stepanyan,<sup>3</sup> I.I. Strakovsky,<sup>5</sup> S. Strauch,<sup>37</sup> A. Thornton,<sup>35</sup> N. Tyler,<sup>37</sup> R. Tyson,<sup>35</sup> M. Ungaro,<sup>3</sup> L. Venturelli,<sup>12,13</sup> H. Voskanyan,<sup>27</sup> E. Voutier,<sup>18</sup> D.P. Watts,<sup>31</sup> K. Wei,<sup>22</sup> X. Wei,<sup>3</sup> M.H. Wood,<sup>49</sup> B. Yale,<sup>1</sup> N. Zachariou,<sup>31</sup> and J. Zhang<sup>40</sup>

(The CLAS Collaboration)

<sup>1</sup>College of William and Mary, Williamsburg, Virginia 23187-8795

<sup>2</sup>Duke University, Durham, North Carolina 27708-0305

<sup>3</sup>Thomas Jefferson National Accelerator Facility, Newport News, Virginia 23606

<sup>4</sup>Florida International University, Miami, Florida 33199

<sup>5</sup>The George Washington University, Washington, DC 20052

<sup>6</sup>University of California, Riverside, Riverside, California, 92521

<sup>7</sup>Temple University, Philadelphia, PA 19122

<sup>8</sup>INFN, Sezione di Ferrara, 44100 Ferrara, Italy

<sup>9</sup>INFN, Sezione di Genova, 16146 Genova, Italy

<sup>10</sup>National Research Centre Kurchatov Institute - ITEP, Moscow, 117259, Russia

<sup>11</sup>Duquesne University, 600 Forbes Avenue, Pittsburgh, PA 15282

<sup>12</sup>Università degli Studi di Brescia, 25123 Brescia, Italy

<sup>13</sup>INFN, Sezione di Pavia, 27100 Pavia, Italy

<sup>14</sup>Fairfield University, Fairfield CT 06824

<sup>15</sup>IRFU, CEA, Université Paris-Saclay, F-91191 Gif-sur-Yvette, France

<sup>16</sup>Universidad Técnica Federico Santa María, Casilla 110-V Valparaíso, Chile

<sup>17</sup>Old Dominion University, Norfolk, Virginia 23529

<sup>18</sup>Université Paris-Saclay, CNRS/IN2P3, IJCLab, 91405 Orsay, France

<sup>19</sup>Mississippi State University, Mississippi State, MS 39762-5167

<sup>20</sup>Ohio University, Athens, Ohio 45701

<sup>21</sup>Università di Ferrara, 44121 Ferrara, Italy

<sup>22</sup>University of Connecticut, Storrs, Connecticut 06269

<sup>23</sup>Lamar University, 4400 MLK Blvd, PO Box 10046, Beaumont, Texas 77710

<sup>24</sup>Florida State University, Tallahassee, Florida 32306

<sup>25</sup>INFN, Sezione di Roma Tor Vergata, 00133 Rome, Italy

<sup>26</sup>Università di Roma Tor Vergata, 00133 Rome Italy

<sup>27</sup>Yerevan Physics Institute, 375036 Yerevan, Armenia

<sup>28</sup>II. Physikalisches Institut der Universität Gießen, 35392 Gießen, Germany

<sup>29</sup>Arizona State University, Tempe, Arizona 85287

<sup>30</sup>Argonne National Laboratory, Argonne, Illinois 60439

<sup>31</sup>University of York, York YO10 5DD, United Kingdom

<sup>32</sup>INFN, Sezione di Torino, 10125 Torino, Italy

<sup>33</sup>Idaho State University, Pocatello, Idaho 83209

<sup>34</sup>University of Richmond, Richmond, Virginia 23173

<sup>35</sup>University of Glasgow, Glasgow G12 8QQ, United Kingdom

<sup>36</sup>Skobeltsyn Institute of Nuclear Physics, Lomonosov Moscow State University, 119234 Moscow, Russia

- <sup>37</sup> *University of South Carolina, Columbia, South Carolina 29208*  
<sup>38</sup> *University of New Hampshire, Durham, New Hampshire 03824-3568*  
<sup>39</sup> *Kyungpook National University, Daegu 41566, Republic of Korea*  
<sup>40</sup> *University of Virginia, Charlottesville, Virginia 22901*  
<sup>41</sup> *Massachusetts Institute of Technology, Cambridge, Massachusetts 02139-4307*  
<sup>42</sup> *Università degli Studi dell'Insubria, 22100 Como, Italy*  
<sup>43</sup> *INFN, Laboratori Nazionali di Frascati, 00044 Frascati, Italy*  
<sup>44</sup> *James Madison University, Harrisonburg, Virginia 22807*  
<sup>45</sup> *New Mexico State University, PO Box 30001, Las Cruces, NM 88003, USA*  
<sup>46</sup> *Christopher Newport University, Newport News, Virginia 23606*  
<sup>47</sup> *Institute für Kernphysik (Juelich), Juelich, Germany*  
<sup>48</sup> *Norfolk State University, Norfolk, Virginia 23504*  
<sup>49</sup> *Canisius College, Buffalo, New York 14208-1098*  
(Dated: April 11, 2024)

The observation of beam spin asymmetries in two-pion production in semi-inclusive deep inelastic scattering off an unpolarized proton target is reported for the first time. The data presented here were taken in the fall of 2018 with the CLAS12 spectrometer using a 10.6 GeV longitudinally spin-polarized electron beam delivered by CEBAF at JLab. The measured asymmetries provide the first observation of a signal that can be used to extract the PDF  $e(x)$  in a collinear framework and the helicity-dependent two-pion fragmentation function  $G_1^\perp$ .

Keywords: dihadron; beam spin asymmetry; SIDIS; CLAS12; twist-3 PDF; dihadron fragmentation function

Protons and neutrons constitute most of the visible matter of the universe, however our understanding of how some of their most important properties, such as mass and spin, emerge from the strong interactions of the constituent quarks and gluons is still incomplete. Therefore, the study of the internal dynamics of the nucleon is fundamental to our understanding of the theory of strong interactions and, by extension, our understanding of the nature of matter itself.

Parton distribution functions (PDFs) encode information about the momentum-dependent distribution of quarks inside the proton. In the approximation of the parton model, PDFs describe the probability of scattering off a specific parton in the nucleon. Comparably, the non-perturbative dynamics of hadronization, the process of the formation of hadrons out of quarks and gluons, are described by fragmentation functions (FFs), which can be interpreted in the parton model as the probability that a quark forms a certain hadron. For recent reviews, see Refs. [1–4].

In order to access PDFs and FFs, we consider the semi-inclusive deep inelastic scattering (SIDIS) process, where an electron scatters off a proton target at a high enough energy such that this process can be described by the scattering off a single parton in the target [3]. This Letter focuses on the measurement of beam spin asymmetries for the two-pion production process in SIDIS, written

$$e(\ell) + p(P) \rightarrow e'(\ell') + \pi^+(P_1) + \pi^-(P_2) + X, \quad (1)$$

where the quantities in the parentheses denote the respective four-momenta; boldface symbols will indicate the corresponding three-momenta. Fragmentation into two pions offers more targeted access to the nucleon structure and allows for the observation of more complex phenomena in fragmentation than in single-pion production [2].

The first measurement of two-pion beam-spin asymmetries sensitive to the PDF  $e(x)$  and to the dihadron FF  $G_1^\perp$  are reported.

Insights into the interaction between gluons and the struck quark in the nucleon can be gained from subleading-twist functions such as  $e(x)$  [5, 6]. For example, the  $x^2$ -moment of  $e(x)$  is proportional to the force experienced by a transversely polarized quark in an unpolarized nucleon immediately after scattering [7, 8]. Like the other collinear PDFs, it is dependent on the scaling variable  $x$ , which in the parton picture corresponds to the light-cone momentum fraction carried by the probed quark [3, 5, 9] and can be expressed as  $x = Q^2/(2P^\mu q_\mu)$ . As usual  $Q^2 = -q^\mu q_\mu$  denotes the scale of the process, where  $q = \ell - \ell'$  is the four-momentum of the exchanged virtual photon.

A first model-dependent extraction of  $e(x)$  from single-hadron data has been performed [10], along with another extraction from preliminary two-pion data from CLAS [11, 12]. In SIDIS single-hadron production,  $e(x)$  can only be accessed via beam spin asymmetries with the inclusion of the transverse momentum dependence (TMD) of the FF. This leads to a convolution of the PDF and FF over the TMD. Furthermore, factorization in the TMD framework is not yet proven at subleading twist [13]. These issues motivate the high-precision measurement of two-pion beam spin asymmetries presented here.

On the hadronization side, FFs describing two-pion production depend on  $M_h$ , the invariant mass of the pion pair and on  $z$ , the fraction of the fragmenting quark momentum carried by the pion pair. Dihadron FFs can be decomposed into partial waves [14, 15], with the corresponding associated Legendre polynomials depending on the decay angle  $\theta$  of the two-hadron system. This de-

pendence is integrated over the CLAS12 acceptance in the results shown in this Letter and the relevant mean  $\theta$  values are listed in the supplementary material.

The dihadron FF  $G_1^\perp$  describes the dependence of the two-pion production on the helicity of the fragmenting quark. Recently, interest in the possible mechanism behind  $G_1^\perp$  led to several model calculations [16, 17]. In Ref. [17] interference between different partial waves leads to a signal with a distinctive dependence on  $M_h$ , with a sign change around the  $\rho$  mass. It is also interesting to note that  $G_1^\perp$  could be sensitive to QCD vacuum fluctuations [18] and thus to the strong CP problem. No previous measurement sensitive to  $G_1^\perp$  exists and the asymmetries given here constitute the first opportunity to study this unique FF.

The data presented in this Letter were taken with the CLAS12 spectrometer [19] using a 10.6 GeV longitudinally polarized electron beam delivered by CEBAF, incident on a liquid-hydrogen target. The beam polarization averaged to  $86.9\% \pm 2.6\%$  and was flipped at 30 Hz to minimize systematic effects. This analysis uses the Forward Detector of CLAS12, which contains a tracking subsystem consisting of drift chambers in a toroidal magnetic field and high and low-threshold Cherenkov counters to identify the scattered electron and final state pions, respectively. Additional identification is performed for electrons with an electromagnetic calorimeter and for pions by six arrays of plastic scintillation counters.

SIDIS events were selected by requiring  $Q^2 > 1 \text{ GeV}^2$  and the mass of the hadronic final state to be above 2 GeV. Exclusive reactions were removed with the condition on the missing mass  $M_X > 1.5 \text{ GeV}$ , defined as the mass of  $X$ , the unmeasured part of the final state. Contributions from events where a photon is radiated from the incoming lepton were reduced by placing a condition of  $y < 0.8$ , where  $y = P^\mu q_\mu / (P^\mu l_\mu)$  is the fractional energy loss of the scattered electron, and by requiring a minimum momentum of 1.25 GeV for each pion. Finally, contributions from the target fragmentation region were reduced by requiring  $x_F > 0$  for each pion, where  $x_F$  denotes Feynman- $x$  and takes a positive value if the outgoing hadron moves in the same direction as the incoming electron, in the struck quark center-of-mass frame.

The correlations between quark and gluon fields in the nucleon encoded in  $e(x)$ , as well as the hadronization process described by  $G_1^\perp$ , are imprinted in the azimuthal angles of the final state hadrons [14, 15, 20]. An observable sensitive to these functions can thus be constructed by analyzing beam helicity-dependent azimuthal modulations of the two-pion cross section as described below. Figure 1 illustrates the two-pion three-momenta  $\mathbf{P}_h = \mathbf{P}_1 + \mathbf{P}_2$  and  $2\mathbf{R} = \mathbf{P}_1 - \mathbf{P}_2$ , where  $\mathbf{P}_1$  is assigned to the  $\pi^+$ ; the azimuthal angles  $\phi_h$  and  $\phi_{R_\perp}$  are

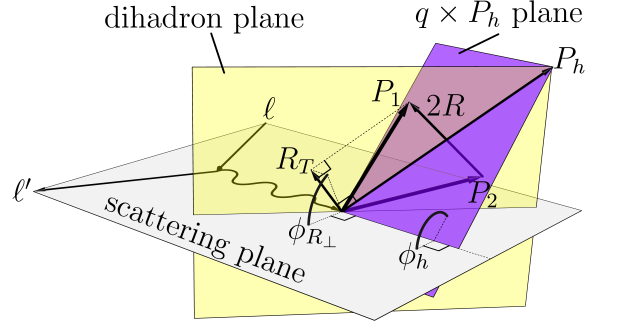


FIG. 1. The coordinate system used in this analysis. The electron scattering plane is spanned by the incoming and outgoing lepton, the dihadron plane is spanned by  $\mathbf{P}_1$  and  $\mathbf{P}_2$ , containing also  $\mathbf{P}_h$ ,  $\mathbf{R}$ , and  $\mathbf{R}_T$ , and the  $\mathbf{q} \times \mathbf{P}_h$  plane contains only  $\mathbf{q}$  and  $\mathbf{P}_h$ . The azimuthal angles  $\phi_h$  and  $\phi_{R_\perp}$  are defined within the plane transverse to  $\mathbf{q}$ , from the electron scattering plane to, respectively, the  $\mathbf{q} \times \mathbf{P}_h$  plane and the dihadron plane. See text for details.

defined as

$$\phi_h = \frac{(\mathbf{q} \times \mathbf{l}) \cdot \mathbf{P}_h}{|(\mathbf{q} \times \mathbf{l}) \cdot \mathbf{P}_h|} \arccos \frac{(\mathbf{q} \times \mathbf{l}) \cdot (\mathbf{q} \times \mathbf{P}_h)}{|\mathbf{q} \times \mathbf{l}| |\mathbf{q} \times \mathbf{P}_h|}, \quad (2)$$

$$\phi_{R_\perp} = \frac{(\mathbf{q} \times \mathbf{l}) \cdot \mathbf{R}_T}{|(\mathbf{q} \times \mathbf{l}) \cdot \mathbf{R}_T|} \arccos \frac{(\mathbf{q} \times \mathbf{l}) \cdot (\mathbf{q} \times \mathbf{R}_T)}{|\mathbf{q} \times \mathbf{l}| |\mathbf{q} \times \mathbf{R}_T|}, \quad (3)$$

where  $\mathbf{R}_T$  is the component of  $\mathbf{R}$  perpendicular to  $\mathbf{P}_h$ , calculated as  $\mathbf{R}_T = (z_2 \mathbf{P}_1^\perp - z_1 \mathbf{P}_2^\perp) / z$  [16].

The beam helicity-dependent part of the two-pion cross section can be written in terms of PDFs and FFs, integrating over partonic transverse momenta at subleading twist as [14, 15, 20]

$$d\sigma_{LU} \propto W \lambda_e \sin(\phi_{R_\perp}) \left( x e(x) H_1^\triangleleft(z, M_h) + \frac{1}{z} f(x) \tilde{G}^\triangleleft(z, M_h) \right) + \dots \quad (4)$$

Here, the subscript  $LU$  refers to a longitudinally polarized beam and an unpolarized target,  $\lambda_e$  is the electron helicity and  $W$  is a kinematic proportionality factor appropriate for the  $LU$  term and dependent on  $x$  and  $y$ , and is interpreted as the depolarization of the exchanged virtual photon [14, 15, 20]. The additional terms are linearly independent of the  $\sin(\phi_{R_\perp})$  term shown here and can therefore be extracted independently. Eq. (4) omits the sum over quark flavors.

The dihadron FF  $H_1^\triangleleft$  that  $e(x)$  is multiplied by is sensitive to the transverse polarization of the outgoing quark and has been extracted from  $e^+e^-$  data [21, 22]. The second term contains the twist-3 dihadron FF  $\tilde{G}^\triangleleft$ , which is significantly smaller than  $H_1^\triangleleft$  in model calculations [23], but remains unmeasured. The two contributions can be disentangled in a combined fit including target spin asymmetries [12].

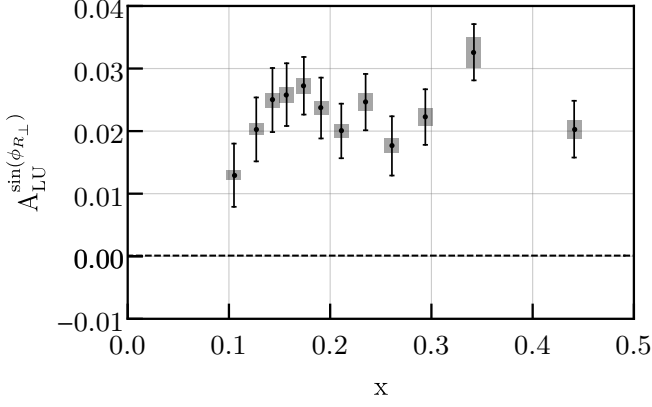


FIG. 2. The measured  $A_{LU}^{\sin(\phi_{R\perp})}$  asymmetry vs.  $x$ . The thin, black bars indicate statistical uncertainties and the vertical extent of the wide, gray bars indicates systematic uncertainties. See text for further discussion.

When the dependence on transverse momenta is included, the cross section depends on  $\phi_h$  and the dihadron FF  $G_1^\perp$  appears, which describes the helicity dependence of the two-pion production:

$$d\sigma_{LU} \propto C\lambda_e \sin(\phi_h - \phi_{R\perp}) \mathcal{I}[f_1 G_1^\perp] + \dots, \quad (5)$$

where  $C$  is the corresponding kinematic depolarization factor and additional terms in the cross section are again linearly independent from the given one. As  $G_1^\perp$  is a TMD FF, it appears in Eq. (5) in a convolution, denoted by  $\mathcal{I}$ , over the transverse momentum dependences of the PDF and FF [14, 15, 24].

The individual terms can be extracted from Eqs. (4) and (5) by forming the beam spin asymmetry  $A_{LU}$  from the two-pion yields  $N^\pm$ , produced from the scattering of an electron with helicity  $\pm$ , written

$$A_{LU} = \frac{1}{P_{\text{beam}}} \frac{N^+(\phi_h, \phi_{R\perp}) - N^-(\phi_h, \phi_{R\perp})}{N^+(\phi_h, \phi_{R\perp}) + N^-(\phi_h, \phi_{R\perp})} = \quad (6)$$

$$A_{LU}^{\sin(\phi_h - \phi_{R\perp})} \sin(\phi_h - \phi_{R\perp}) + A_{LU}^{\sin(\phi_{R\perp})} \sin(\phi_{R\perp}),$$

and fitting for the resulting azimuthal modulation amplitudes where  $P_{\text{beam}}$  is the beam polarization. The amplitudes in Eq. (6) were extracted from the data using an unbinned maximum likelihood fit that includes additional modulations beyond the two listed here, from the cross section partial waves up to  $\ell = 2$ ; see Ref. [15] for details. A binned  $\chi^2$ -minimization fit with  $8 \times 8$  bins in  $\phi_h$  and  $\phi_{R\perp}$  was also performed and is in very good agreement with the unbinned fit with a mean reduced  $\chi^2$  of 1.05. The resulting asymmetries are corrected for the ratio of the depolarization factors  $W(x, y)$  and  $C(x, y)$  in Eqs. (4) and (5) to the respective factor  $A(x, y)$  of the unpolarized cross section.

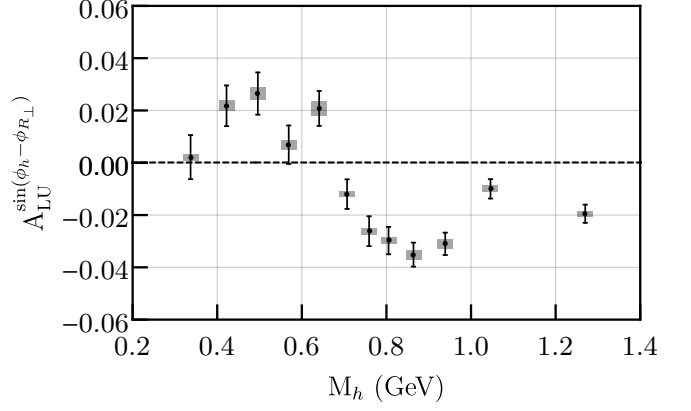


FIG. 3. The measured  $A_{LU}^{\sin(\phi_h - \phi_{R\perp})}$  asymmetry vs.  $M_h$ . The thin, black bars indicate statistical uncertainties and the vertical extent of the wide, gray bars indicates systematic uncertainties. See text for further discussion.

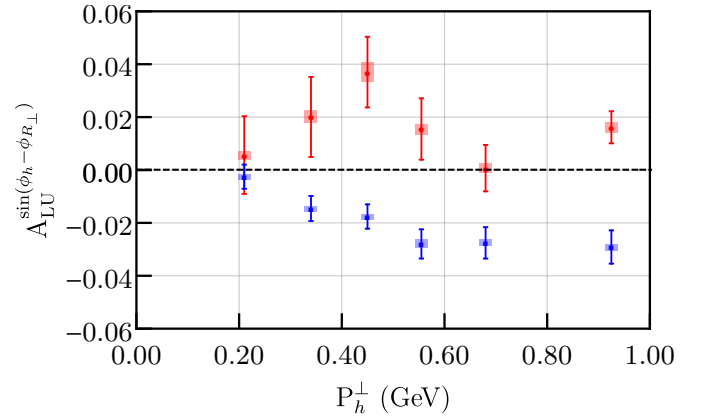


FIG. 4. The measured  $A_{LU}^{\sin(\phi_h - \phi_{R\perp})}$  asymmetry vs.  $P_h^\perp$ . The data have been split into two bins of  $M_h$  above and below 0.63 GeV. Asymmetries for lower values of  $M_h$  are shown in red squares and the blue circles show the values for higher  $M_h$ . The thin, solid bars indicate statistical uncertainties and the vertical extent of the wide bars indicates systematic uncertainties. See text for further discussion.

Figure 2 shows the result for  $A_{LU}^{\sin(\phi_{R\perp})}$  vs.  $x$  and integrated over the other relevant variables. A significant signal is observed that is relatively flat throughout the valence quark region. The PDF  $e(x)$  is confirmed to be nonzero and its general shape can be observed because the asymmetry presented here is proportional to  $e(x)H_1^\perp(z, M_h)$  and  $H_1^\perp(z, M_h)$  is well-constrained [12]. The function  $e(x)$  can be extracted point-by-point from these data with further theoretical development.

In Figs. 3-5 results for  $A_{LU}^{\sin(\phi_h - \phi_{R\perp})}$ , sensitive to  $G_1^\perp$ , are shown vs.  $M_h$ ,  $P_h^\perp$  and  $z$  and integrated over the other variables. The quantity  $P_h^\perp$ , the transverse momentum of the final-state pion pair with respect to  $\mathbf{q}$ , accesses the convolution of the TMD of the PDF and dihadron FF.

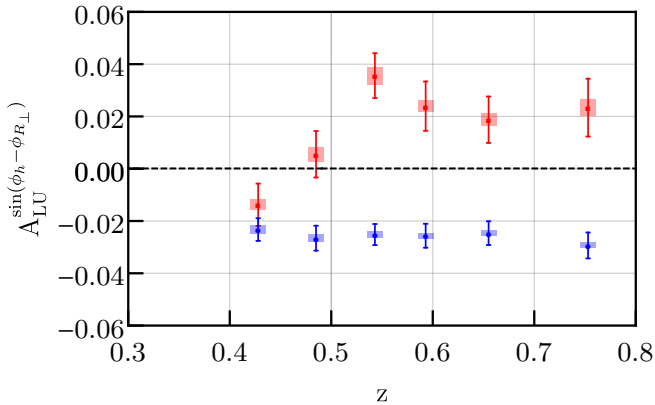


FIG. 5. The measured  $A_{LU}^{\sin(\phi_h - \phi_{R\perp})}$  asymmetry vs.  $z$ . The data have been split into two bins of  $M_h$  above and below 0.63 GeV. Asymmetries for lower values of  $M_h$  are shown in red squares and the blue circles show the values for higher  $M_h$ . The thin, solid bars indicate statistical uncertainties and the vertical extent of the wide bars indicates systematic uncertainties. See text for further discussion.

In particular, a dependence on  $M_h$  with a sign change around the  $\rho$  mass is seen. This behavior is consistent with model calculations [17] and originates from the real part of the interference of  $s$  and  $p$  wave dihadrons.

Inspired by the sign change in  $M_h$ , the data were further split into events with  $M_h < 0.63$  GeV and  $M_h > 0.63$  GeV to investigate the dependence on  $z$  and on  $P_h^\perp$ . The dependence on  $P_h^\perp$  is of special interest, since here for the first time results are shown that are sensitive to a TMD fragmentation into two pions. It is a common assumption that the transverse momentum dependence of the PDFs and FFs is Gaussian [3]; the data are consistent with this assumption but with an indication for different widths in the two mass regions. One interpretation is that for  $M_h > 0.63$  GeV, vector mesons make up a significant fraction of the hadron pairs, which changes the transverse momentum spectrum. This interpretation would also be relevant in single-hadron production. Finally, the dependence of the asymmetry on  $z$ , shown in Fig. 5, is relatively flat for both  $M_h$  bins with the exception of  $z < 0.5$  for the lower  $M_h$  bin, where the asymmetry is smaller and may change sign at the lowest  $z$  value.

Systematic effects on these measurements have been studied using a Monte Carlo simulation based on the PEPSI generator [25] and a GEANT4-based simulation of the detector [26, 27] that was tuned to match the CLAS12 data. The systematic uncertainties are dominated by contributions from baryonic decays from the target fragmentation region, bin migration effects, and a scale uncertainty stemming from the uncertainty on the beam polarization. Baryonic contributions from the target fragmentation region are dependent on  $z$ , reaching up to 6% at the lowest  $z$  but falling steeply to about

1% at  $z$  of 0.755. Bin migration effects are only significant for  $A_{LU}^{\sin(\phi_h - \phi_{R\perp})}$ , which changes rapidly around the  $\rho$  mass. In this region, systematic uncertainties from bin migration reach up to 10% of the asymmetry. The beam polarization scale uncertainty is 3.0%.

Several additional sources of systematic uncertainties have been studied but found to be negligible. Contributions include particle identification, radiative effects, accidental coincidences and the photoproduction of electrons that are misidentified as the scattered electron.

Eqs. (4) and (5) show the beam-spin dependent part of the cross section, however, the asymmetries  $A_{LU}$  are normalized by the beam-spin independent cross section  $\sigma_{UU}$ . The unknown relative strength of the partial waves contributing to  $\sigma_{UU}$ , along with their non-orthogonality within the experimental acceptance, leads to an effective shift in the extracted asymmetries. The size of this effect has been estimated elsewhere [28], but a precise systematic assignment requires a more thorough understanding of the unpolarized fragmentation function than is currently available. The supplementary materia contains estimates of the effect on  $A_{LU}$  based on Monte Carlo studies, however these estimates are based on an assumption of the size of the yet unknown  $\sigma_{UU}$  modulation amplitudes and are therefore not included in the presented systematic uncertainties.

In summary, this Letter reports the first significant beam spin asymmetries observed in two-pion production in SIDIS. The data indicate a non-zero signal for the azimuthal modulation sensitive to the subleading-twist PDF  $e(x)$  and, with further theoretical development, will enable a point-by-point extraction of this quantity. Additionally, the first measurement sensitive to  $G_1^\perp$ , the helicity-dependent dihadron FF is reported. Figures 2–5 show the main results, and all asymmetry measurements are included in the CLAS Physics Database [29]. Future work will concentrate on a measurement of the partial wave decomposition of  $\sigma_{LU}$  and  $\sigma_{UU}$ , which will address the uncertainty discussed above but is also interesting in its own right in order to gain further insight into hadronization phenomena as well. The beam spin asymmetry modulated by  $\sin(\phi_h)$ , which has been a byproduct of the extraction presented here, will be a topic of future studies. It can be thought of as the equivalent to the Collins FF for two pions [18] and, in the  $\rho$  mass region, can be used to test predictions by the Artru model about the relative size of Collins asymmetries of vector and scalar mesons [30].

We acknowledge the outstanding efforts of the staff of the Accelerator and the Physics Divisions at Jefferson Lab in making this experiment possible. This work was supported in part by the U.S. Department of Energy, the National Science Foundation (NSF), the Italian Istituto Nazionale di Fisica Nucleare (INFN), the French Centre National de la Recherche Scientifique (CNRS), the

French Commissariat pour l'Energie Atomique, the UK Science and Technology Facilities Council, the National Research Foundation (NRF) of Korea, the Helmholtz-Forschungsakademie Hessen für FAIR (HFHF) and the Ministry of Science and Higher Education of the Russian Federation. The Southeastern Universities Research Association (SURA) operates the Thomas Jefferson National Accelerator Facility for the U.S. Department of Energy under Contract No. DE-AC05-06OR23177. TH thanks the Department of Energy for support under grant DE-FG02-96ER41003.

---

\* Current address: Università degli Studi di Brescia, 25123 Brescia, Italy

- [1] C. A. Aidala, S. D. Bass, D. Hasch, and G. K. Mallot, *Rev. Mod. Phys.* **85**, 655 (2013), arXiv:1209.2803 [hep-ph].
- [2] A. Metz and A. Vossen, *Prog. Part. Nucl. Phys.* **91**, 136 (2016), arXiv:1607.02521 [hep-ex].
- [3] M. Anselmino, A. Mukherjee, and A. Vossen, *Prog. Part. Nucl. Phys.* **114**, 103806 (2020), arXiv:2001.05415 [hep-ph].
- [4] H. Avakian, B. Parsamyan, and A. Prokudin, *Riv. Nuovo Cim.* **42**, 1 (2019), arXiv:1909.13664 [hep-ex].
- [5] A. Efremov and P. Schweitzer, *JHEP* **08**, 006 (2003), arXiv:hep-ph/0212044.
- [6] C.-Y. Seng, *Phys. Rev. Lett.* **122**, 072001 (2019), arXiv:1809.00307 [hep-ph].
- [7] M. Burkardt, *Phys. Rev. D* **88**, 114502 (2013), arXiv:0810.3589 [hep-ph].
- [8] B. Pasquini and S. Rodini, *Phys. Lett. B* **788**, 414 (2019), arXiv:1806.10932 [hep-ph].
- [9] R. Jaffe and X.-D. Ji, *Phys. Rev. D* **43**, 724 (1991).
- [10] A. Efremov, K. Goeke, and P. Schweitzer, *Phys. Rev. D* **67**, 114014 (2003), arXiv:hep-ph/0208124.
- [11] M. Mirazita *et al.* (CLAS Collaboration), (2020), arXiv:2010.09544 [hep-ex].
- [12] A. Courtoy, (2014), arXiv:1405.7659 [hep-ph].
- [13] A. Bacchetta, G. Bozzi, M. G. Echevarria, C. Pisano, A. Prokudin, and M. Radici, *Phys. Lett. B* **797**, 134850 (2019), arXiv:1906.07037 [hep-ph].
- [14] A. Bacchetta and M. Radici, *Phys. Rev. D* **67**, 094002 (2003), arXiv:hep-ph/0212300.
- [15] S. Gliske, A. Bacchetta, and M. Radici, *Phys. Rev. D* **90**, 114027 (2014), [Erratum: *Phys. Rev. D* **91**, 019902 (2015)], arXiv:1408.5721 [hep-ph].
- [16] H. H. Matevosyan, A. Kotzinian, and A. W. Thomas, *Phys. Rev. D* **96**, 074010 (2017), arXiv:1707.04999 [hep-ph].
- [17] X. Luo, H. Sun, and Y.-L. Xie, *Phys. Rev. D* **101**, 054020 (2020), arXiv:2003.03770 [hep-ph].
- [18] D. Boer, R. Jakob, and M. Radici, *Phys. Rev. D* **67**, 094003 (2003), [Erratum: *Phys. Rev. D* **98**, 039902 (2018)], arXiv:hep-ph/0302232.
- [19] V. D. Burkert *et al.* (CLAS Collaboration), *Nucl. Instrum. Meth. A* **959**, 163419 (2020).
- [20] A. Bacchetta and M. Radici, *Phys. Rev. D* **69**, 074026 (2004), arXiv:hep-ph/0311173.
- [21] A. Vossen *et al.* (Belle Collaboration), *Phys. Rev. Lett.* **107**, 072004 (2011), arXiv:1104.2425 [hep-ex].
- [22] A. Courtoy, A. Bacchetta, M. Radici, and A. Bianconi, *Phys. Rev. D* **85**, 114023 (2012), arXiv:1202.0323 [hep-ph].
- [23] W. Yang, X. Wang, Y. Yang, and Z. Lu, *Phys. Rev. D* **99**, 054003 (2019), arXiv:1902.07889 [hep-ph].
- [24] H. H. Matevosyan, A. Kotzinian, and A. W. Thomas, *Phys. Rev. Lett.* **120**, 252001 (2018), arXiv:1712.06384 [hep-ph].
- [25] L. Mankiewicz, A. Schafer, and M. Veltri, *Comput. Phys. Commun.* **71**, 305 (1992).
- [26] S. Agostinelli *et al.* (GEANT4), *Nucl. Instrum. Meth. A* **506**, 250 (2003).
- [27] M. Ungaro *et al.*, *Nucl. Instrum. Meth. A* **959**, 163422 (2020).
- [28] A. Airapetian *et al.* (HERMES Collaboration), *JHEP* **06**, 017 (2008), arXiv:0803.2367 [hep-ex].
- [29] CLAS Physics Database, <https://clas.sinp.msu.ru/cgi-bin/jlab/db.cgi>.
- [30] X. Artru, (2010), arXiv:1001.1061 [hep-ph].